Supplemental Material

Proton pump inhibitors accelerate endothelial senescence

Authors: Gautham Yepuri PhD, Roman Sukhovershin MD,PhD, Timo Z Nazari-Shafti MD, Michael Petrascheck PhD, Yohannes T. Ghebre, John P. Cooke MD,PhD*

* **Corresponding author:** John P. Cooke, Department of Cardiovascular Sciences, Center for Cardiovascular Regeneration, Houston Methodist Research Institute, 6670 Bertner Ave., Mail Stop: R10-South, Houston, Texas, USA 77030. Email: jpcooke@houstonmethodist.org   Ph: 713.441.8322   Fax: 713.441.7196

This .doc file includes:

Materials and methods
Online Figures I - VIII
Online Tables I - II

Materials and Methods

1. Cell culture.

We cultured human microvascular endothelial cells (ECs) purchased from Lonza (cat # CC-2543) continuously for three passages from passage (P) 4 to P6 in the presence of clinically relevant doses of esomeprazole[1, 2] or vehicle (DMSO). All *in vitro* experiments were performed at P6 upon confluency. ECs were cultured and maintained in EBM-2 Basal Medium (cat # CC-3156) supplemented with EGM-2 MV SingleQuots™ Kit – growth factors, cytokines, and antibiotics (cat # CC-4147).

2. Lysosomal studies.

Cellular pH, lysosomal cathepsin B and protein aggregation were measured in live ECs using pHrodo™ Green/Red dextran, 10,000 MW dye (cat: P35368/P35372, molecular probes®, Life Technologies™), Magic Red™ Cathepsin B Assay Kit (cat: 938, ImmunoChemistry Technologies LLC.) and PROTEOSTAT® Protein aggregation assay (cat: ENZ-51023-KP002, Enzo Life Sciences, Inc.). The pHrodo™ Green dextran when endocytosed permits visualization of endosomal pH, with an inverse non-linear relationship of fluorescence intensity to pH. We confirmed these studies with pHrodo™ Red dextran which provided qualitatively similar findings. All experiments were performed according to manufacturer's user guide. Fluorescence images were taken using Olympus IX51 Inverted fluorescence microscope at 10X magnification and 40X for protein aggregation. All images were quantified using NIH ImageJ 1.47v software. Acid phosphate and N-Acetyl-β-D-Glucosaminidase activity were measured using kits from Sigma-Aldrich, Inc. (cat: CS0740 and CS0780). Cells were harvested using CelLytic™ M (cat: C2978, Sigma-Aldrich, Inc.); fresh cell lysate was used for all experiments. Assay and interpretation of results was performed using manufacturer's instructions. Absorbance was measured using Tecan Infinite® M1000 PRO multimode reader at 405nm.

3. Measurement of superoxide and nitric oxide.

We measured superoxide and nitric oxide in ECs using live cell imaging dyes; DHE (Molecular Probes® cat # D-1168) for superoxide and DAF-2DA (Sigma cat # 50277) for nitric oxide measurement according to the published protocol.[3] Several images per well were captured using Olympus IX51 Inverted fluorescence microscope. Relative fluorescence intensities of images were quantified using NIH ImageJ software. We also assessed the total NO concentration (NOx) using the Griess colorimetric assay as previously described.[4]

4. Assessment of cell proliferation by RTCA and BrdU assay.

We assessed cell proliferation using two different approaches **1.** We analyzed EC proliferation by measuring cell index (CI; an impedance measurement correlated with cell proliferation) using the instrument xCELLigence Real-Time Cell Analyzer (RTCA)[5] developed by ACEA Biosciences, Inc. Experiments were performed according to manufacturer's instructions. In brief, confluent ECs that had been treated with esomeprazole or vehicle for three passages were dissociated using TrypLE™ Express (gibco® by Life Technologies cat # 12605). 10000 cells/well were plated and maintained for 115-120 hours in the xCELLigence RTCA. Later, the CI values were plotted and represented as area under the curve. **2.** We also assessed cell proliferation by using the CytoSelect™ BrdU Cell Proliferation ELISA Kit from Cell Biolabs, Inc. (Cat: CBA-251). The protocol was performed according to manufacturer's instructions. Colorimetric detection of signal was obtained using Tecan Infinite® M1000 PRO multimode reader at absorbance wavelength 450nm.

5. Network formation assay to measure angiogenic capacity.

In order to assess angiogenic capacity of ECs, we used growth factor reduced matrigel from BD Biosciences (cat # 354230). In brief, 24 well flat transparent plates were coated with 200μl of

matrigel/well and allowed to set at 37°C for one hour. Subsequently, 1×10^5 cells/well were seeded and allowed to incubate for 16 hours at 37°C. Several images per well were obtained using Olympus IX51 Inverted fluorescence and bright field microscope. Network branching was quantified using NIH ImageJ software. Total length is equal to the summed length of all segments, branches and isolated branches not within the main network. Total branching length equals the summed length of total segments and total branches within the main network. Total segment length is the summed length of all the segments within the network without branching length.

6. Senescence-associated β-galactosidase (SA-β-gal) staining.

Senescence of ECs was measured using the Cellular Senescence Assay kit from Cell Biolabs, Inc. (Cat: CBA-230). The protocol was performed according to the manufacturer's guide. Briefly, ECs treated continuously for 3 passages with esomeprazole or vehicle were plated in a 6 well plate. Upon confluency, cells were initially fixed and later incubated with SA-β-gal working solution for 16 hours in a non-humidified CO_2 free incubator at 37°C. After incubation the cells were counter stained with SYTO® GREEN fluorescent nucleic acid stain. Several random images per well were taken using light and fluorescent microscope. The SA-β-gal positive cells were counted manually and total cell number per field was quantified using NIH ImageJ software.

7. Long term studies of endothelial histology.

After ECs were exposed to vehicle or ESO (5 or 10uM) through 3 passages (P4-P6), the treatment with ESO or vehicle was discontinued when the cells reached confluency at P6. Subsequently the cells in all groups were maintained in endothelial growth medium which was routinely replaced with fresh medium every 48 hours for 81 days. Microphotographs were taken at regular intervals throughout, and on the final day of culture.

8. Western blot analysis.

Preparation of cell lysate, SDS-PAGE, transfer of proteins onto membrane and western blotting was performed as described previously.[6] To detect PAI-1 protein expression anti-PAI-1 rabbit monoclonal antibody (Cell Signaling Technology, Inc. cat # 11907S) was used and anti-α-Tubulin mouse monoclonal antibody (Sigma cat # T5168) was used to normalize expression.

9. Quantitative PCR and PCR array.

We isolated total RNA from cultured cells using PerfectPure RNA Cultured Cell Kit-50 from 5 PRIME (cat# 2900319) according to the manufacturer's instruction. Complementary DNA (cDNA) was prepared using qScript™ cDNA SuperMix (Quanta BioSciences, Inc. cat # 95048). Quantitative PCR (qPCR) was performed using Taqman gene expression assays (Applied Biosystems). All genes analyzed for expression (listed in the table below) were normalized to GAPDH expression and expressed as relative fold changes using the ΔCt method of analysis. Gene expression of shelterin complex genes was quantified using SYBR™ Green Real Time PCR master mix. Primers for genes related to shelterin complex were obtained from Integrated DNA Technologies, Inc. and are listed in the table below. RT² Profiler PCR Array (Qiagen) was used to assess expression of selected genes associated with specific cellular functions following manufacturer's instructions. Name, catalog numbers and genes detected by the arrays are listed below.

Taqman genes (human) and catalog number used for qPCR

SL #	gene name	Catalog #
1	SERPINE1/PAI-1	Hs01126606_m1
2	CDKN1A(p21)	Hs00355782_m1
3	COL1A1	Hs00164004_m1
4	vWF	Hs01109446_m1
5	DDAH1	Hs00201707_m1
6	DDAH2	Hs00967863_g1
7	eNOS	Hs01574659_m1
8	iNOS	Hs01075529_m1
9	SMAD3	Hs00969210_m1
10	Twist1	Hs00361186_m1
11	GAPDH	Hs02758991_g1

Primers and sequence information for shelterin complex genes

SL #	Gene	primer sequence	
		Sense	**Antisense**
1	TRF1	TCTGCGGTAACTGAATCCTC	GTTACCGGCTGACTCTTTGA
2	TRF2	AGACTTGGGTGGAAGAGGA	TAATCATCACAGCTGTTCGG
3	POT1	TGTGGCAAGATCTCTGAAGG	TCTGAATGCTGATTGGCTGT
4	TPP1	GGGAGGACCAGGAGCAT	GGGCCTAGAGAGCTCAGAAT
5	TIN2	TTGCCTGGAGACAATATGGT	GTCGGCCAGCTAGAGGTT
6	RAP1	GCCACCCGGGAGTTTGA	GGGTGGATCATCATCACACAT

RT² Profiler PCR Array (human) QIAGEN

SL #	Pathway	catalog #
1	Cellular Senescence	PAHS-050Z
2	Epithelial-Mesenchymal Transition	PAHS-090Z
3	TGFß BMP Signaling Pathway	PAHS-035Z
4	Angiogenesis	PAHS-024Z
5	Endothelial Cell Biology	PAHS-015Z

10. Telomere length and telomerase activity.

Telomere length in ECs was measured using monochrome multiplex qPCR (MMqPCR) assay as described previously[7]. The telomeric repeat amplification protocol (TRAP) was performed using TRAPeze® Telomerase Detection Kit (EMD Millipore Inc. cat # S7700). Experiment was performed according to the manufacturer's instructions. In brief, ECs treated with esomeprazole or vehicle were collected, counted and total protein was isolated from 100,000 cells. The amount of

lysate used per reaction was normalized to the amount of 1,000 cells for ECs and 500 cells for telomerase positive control (PC). In short, TRAP was performed at 30°C for 30 minutes and resulting products were amplified in a 29 cycle PCR reaction. Heat inactivated (hi) lysate samples for each condition were used as internal negative controls.

11. Statistical analysis.
All data, unless stated otherwise, was analyzed using GraphPad PRISM 6 software (GraphPad, La Jolla, CA). *n* represents average of 2-3 technical replicates. One-way ANOVA was used for multiple comparisons followed by Bonferroni posthoc correction. The differences between vehicle and treatment groups in each subgroup was analyzed using unpaired t test. All data is expressed as mean ± SEM. Group differences were considered statistically significant at $p < 0.05$.

References

1. http://www.accessdata.fda.gov/drugsatfda_docs/label/2014/022101s014021957s017021153s050lbl.pdf.

2. Shin JM, Kim N. Pharmacokinetics and pharmacodynamics of the proton pump inhibitors. *Journal of neurogastroenterology and motility*. 2013;19:25-35

3. Yepuri G, Velagapudi S, Xiong Y, Rajapakse AG, Montani JP, Ming XF, Yang Z. Positive crosstalk between arginase-ii and s6k1 in vascular endothelial inflammation and aging. *Aging cell*. 2012;11:1005-1016

4. Ghebremariam YT, Yamada K, Lee JC, Johnson CL, Atzler D, Anderssohn M, Agrawal R, Higgins JP, Patterson AJ, Boger RH, Cooke JP. Fxr agonist int-747 upregulates ddah expression and enhances insulin sensitivity in high-salt fed dahl rats. *PloS one*. 2013;8:e60653

5. Ramis G, Martinez-Alarcon L, Quereda JJ, Mendonca L, Majado MJ, Gomez-Coelho K, Mrowiec A, Herrero-Medrano JM, Abellaneda JM, Pallares FJ, Rios A, Ramirez P, Munoz A. Optimization of cytotoxicity assay by real-time, impedance-based cell analysis. *Biomedical microdevices*. 2013;15:985-995

6. Rajapakse AG, Yepuri G, Carvas JM, Stein S, Matter CM, Scerri I, Ruffieux J, Montani JP, Ming XF, Yang Z. Hyperactive s6k1 mediates oxidative stress and endothelial dysfunction in aging: Inhibition by resveratrol. *PloS one*. 2011;6:e19237

7. Ramunas J, Yakubov E, Brady JJ, Corbel SY, Holbrook C, Brandt M, Stein J, Santiago JG, Cooke JP, Blau HM. Transient delivery of modified mrna encoding tert rapidly extends telomeres in human cells. *FASEB journal : official publication of the Federation of American Societies for Experimental Biology*. 2015;29:1930-1939

Online figure I
Showing high power view of lysosomal distribution of pHrodo™ red in vehicle treated and esomeprazole (ESO) treated cells. Fluorescence is reduced in ESO treated cells consistent with an increase in lysosomal pH.

Online figure II
Esomeprazole does not impair NAG activity. β- N-Acetylglucosaminidase activity assay (n=4).

Online figure III
Esomeprazole decreases expression of genes related to NO signaling. (**A-D**) Expression of DDAH1/2, eNOS and iNOS as detected by RT-PCR (n=4-6). *p< 0.05 ESO vs vehicle (DMSO).

Online figure IV
Esomeprazole reduces cell proliferation. Measurement of cell proliferation using real time cell analyzer which generates cell index (CI) values represented as area under curve. EC treated continuously with esomeprazole (ESO; 1uM) for 3 passages (P4-6) manifested a reduction in cell proliferation by comparison to vehicle treated cells.

Online figure V

Ranitidine does not accelerate endothelial senescence. (**A**) Senescent cell number as detected by staining for senescence associated-β-galactosidase (SA-β-gal; upper panel) and for SYTO-13 to detect cell nuclei for total cell count (lower panel). (**B and C**) Respective quantification for % positive SA-β-gal cells and average cell count per field (n=4).

Online figure VI
ESO increases expression of genes related to EndoMT signaling. (**A-D**) EC expression of vwF, SMAD3, TWIST1 and COL1A1 by RT-PCR (n=4-6). *p< 0.05 ESO vs vehicle (DMSO).

Online figure VII
Esomeprazole accelerates EndoMT. Images of ECs treated with chronic exposure (3 passages; P4-P6) **to ESO or vehicle,** and then maintained for 81 days in endothelial growth medium without drugs or vehicle. Cells that were exposed to ESO during passage 4-6 manifest an acceleration of EndoMT in the absence of drug.

Online figure VIII
Absence of telomerase activity in ECs. Telomerase activity as assessed by telomeric repeat amplification protocol assay (n=2).
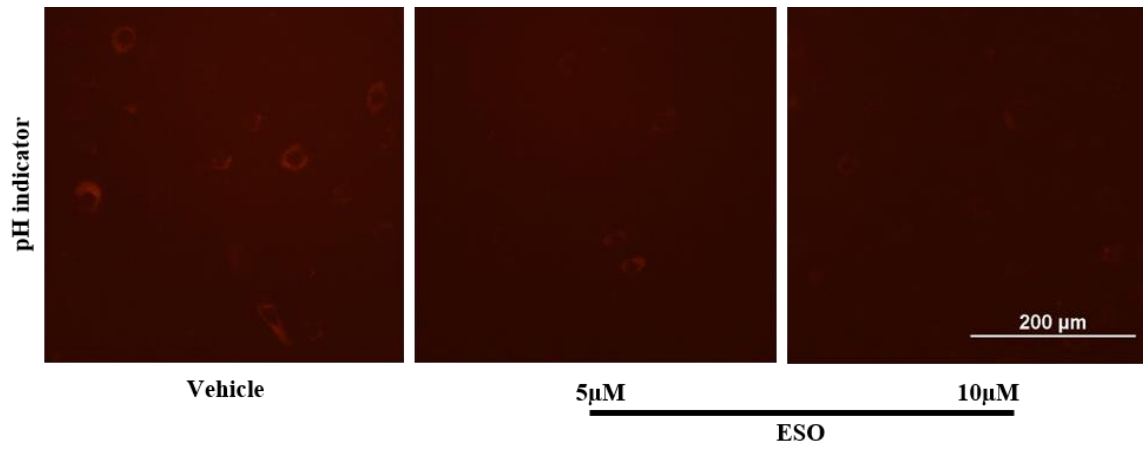
Online table I
Expression of genes (PCR array) that are strongly up regulated (>2 fold) upon treatment with esomeprazole compared to vehicle (DMSO)
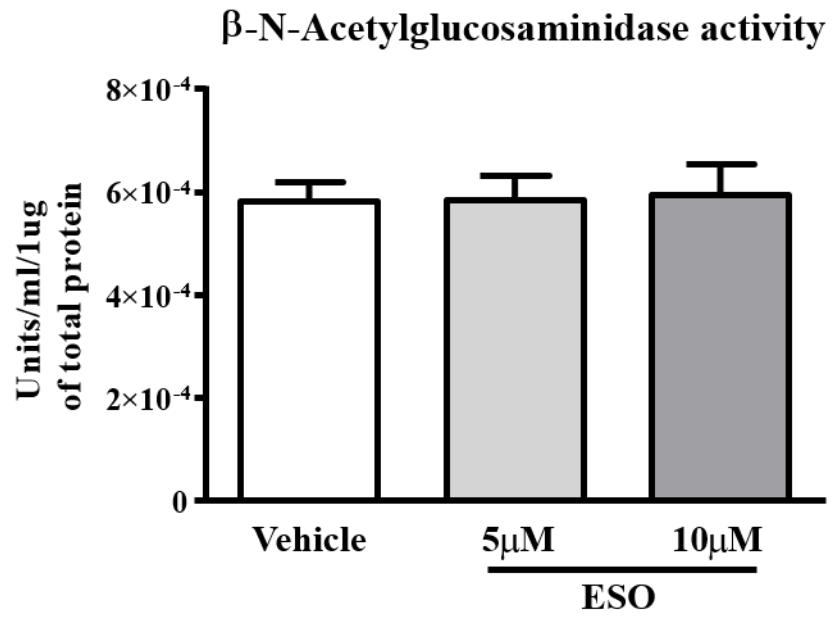
Online table II
Expression of genes (PCR array) that are strongly down regulated (>0.5 fold of control value) upon treatment with esomeprazole compared to vehicle (DMSO)
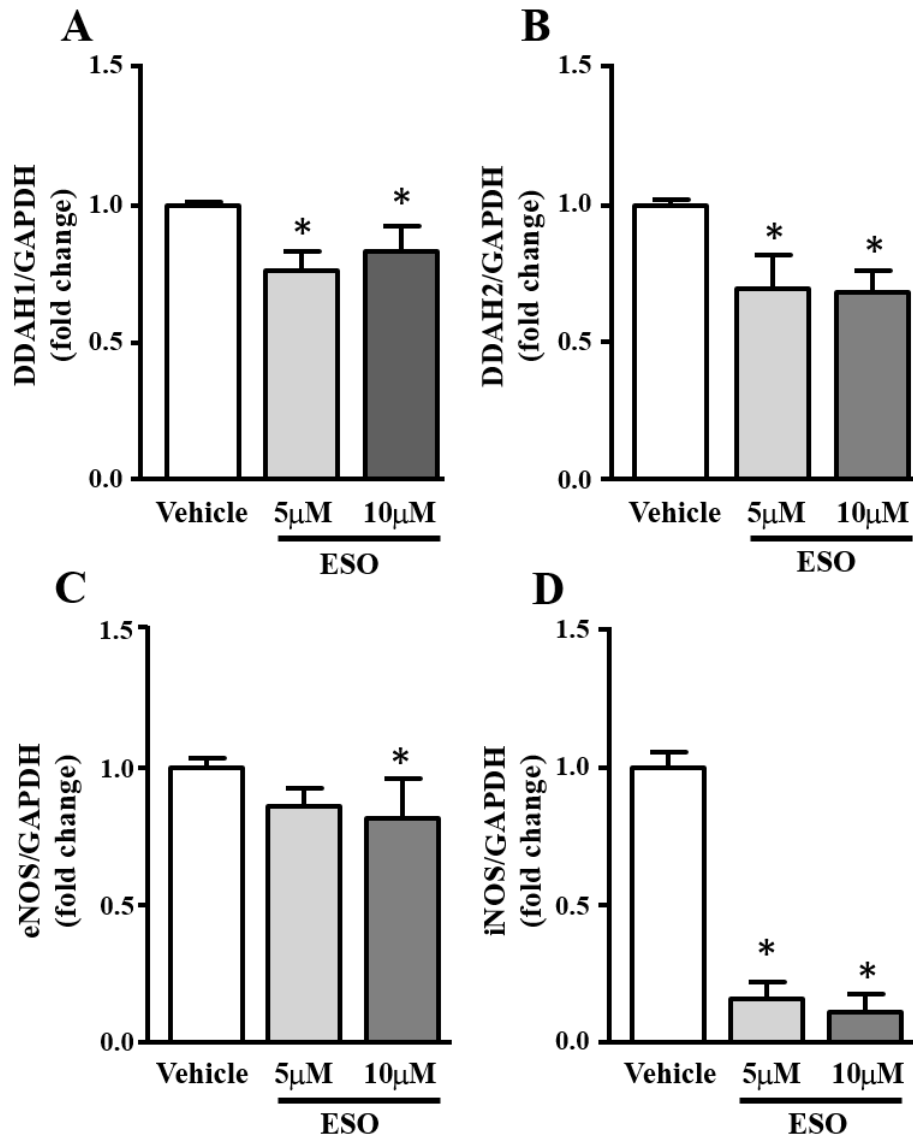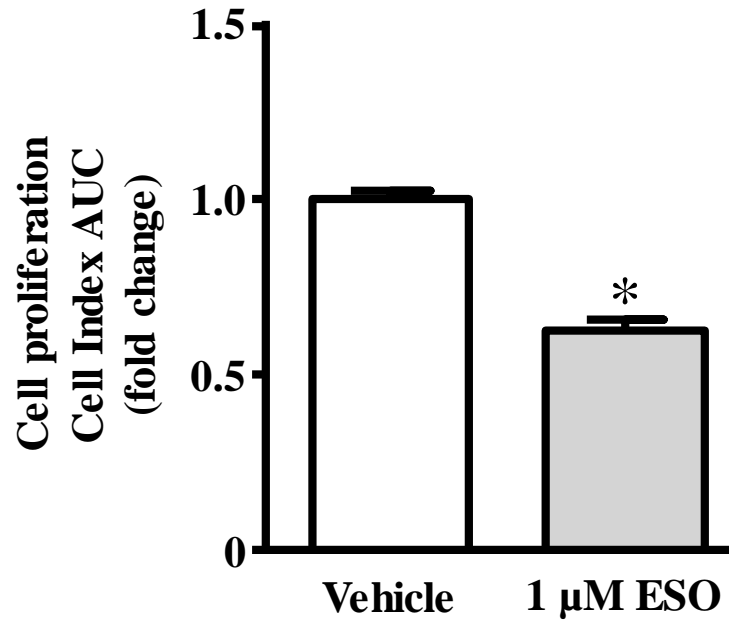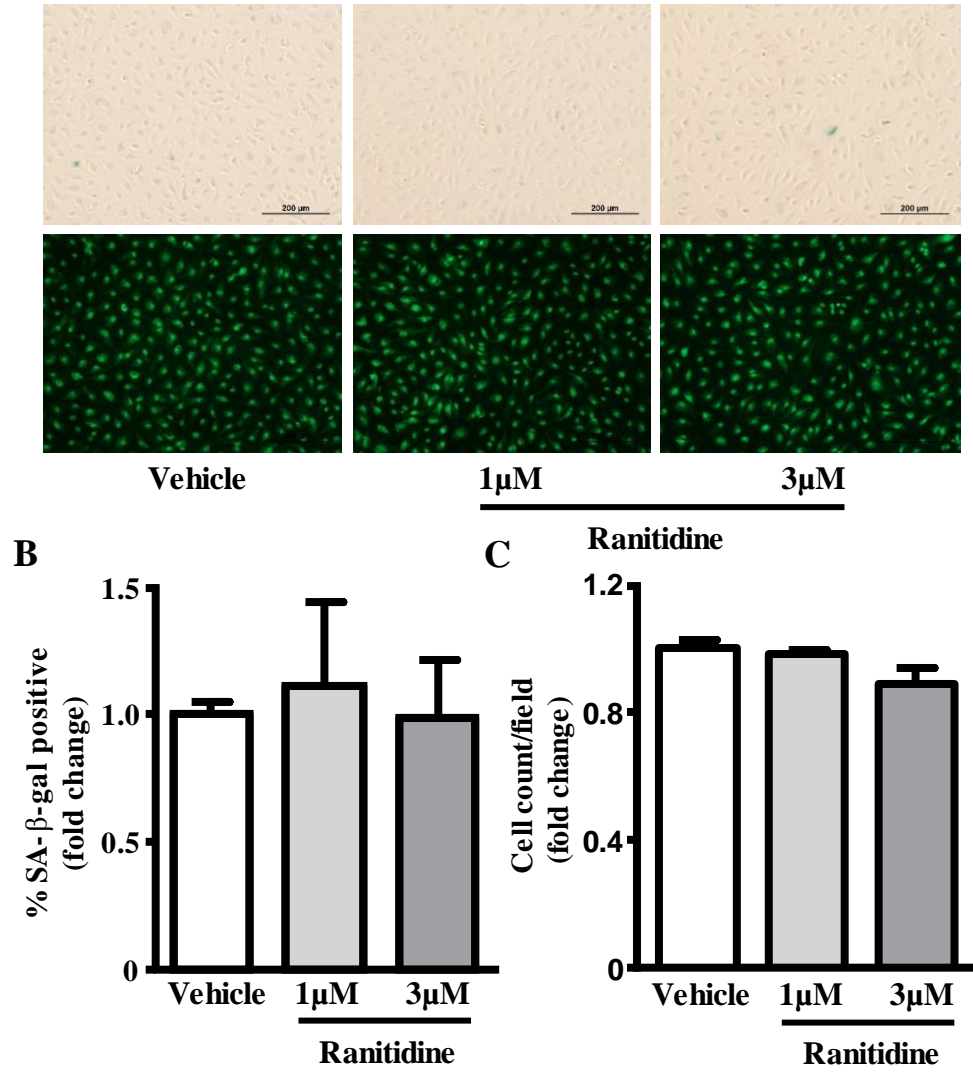
Online Figure I

pH indicator

Vehicle

5μM   10μM

ESO

200 μm

Online figure II

β-N-Acetylglucosaminidase activity
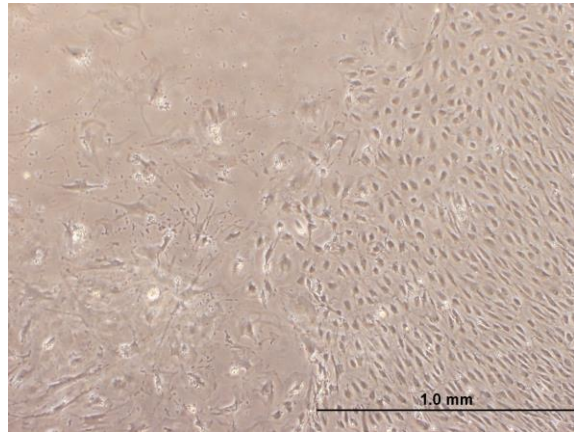
Online figure III

Online figure IV

Online figure V

Online figure VI
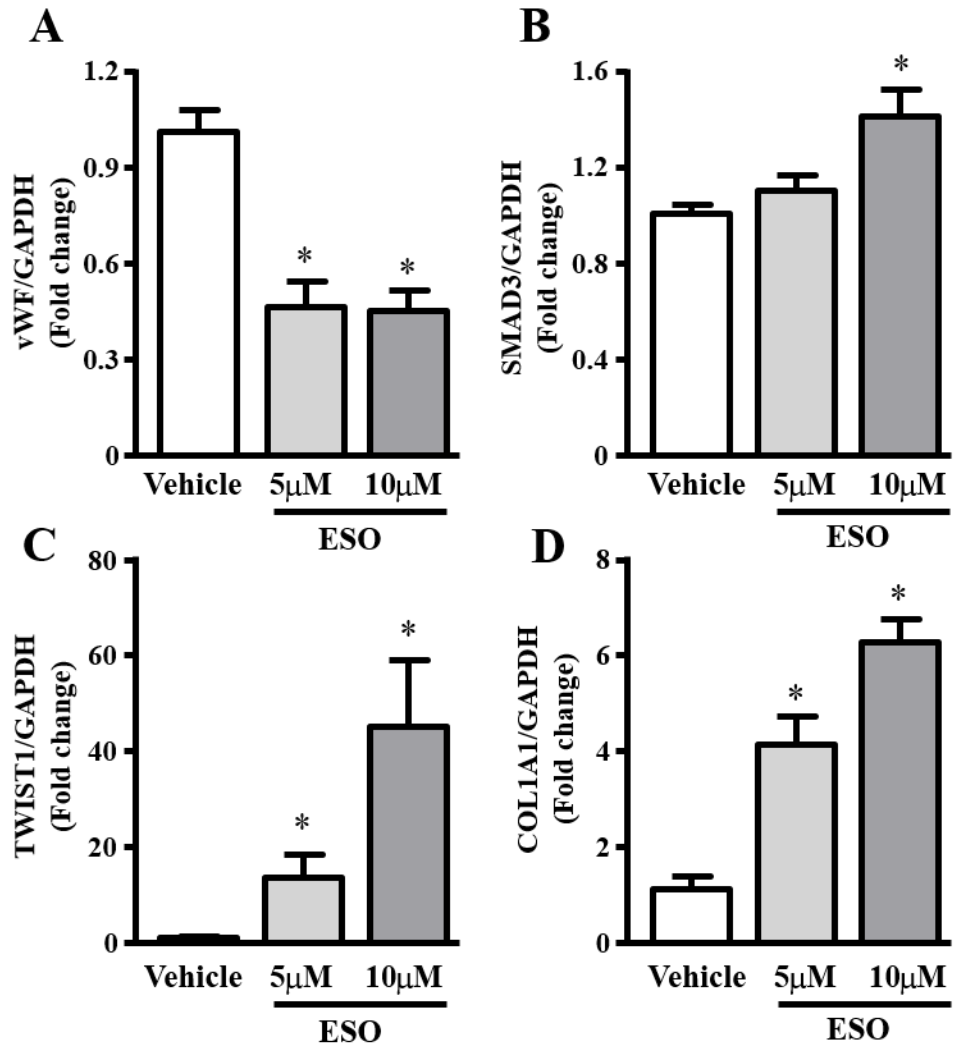
Online figure VII
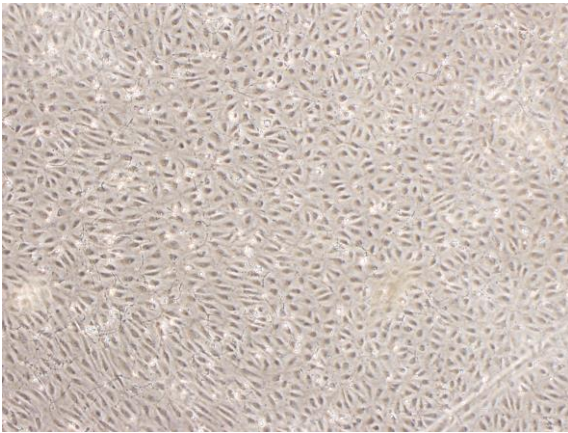
| Vehicle | 5µM ESO |

Online figure VIII
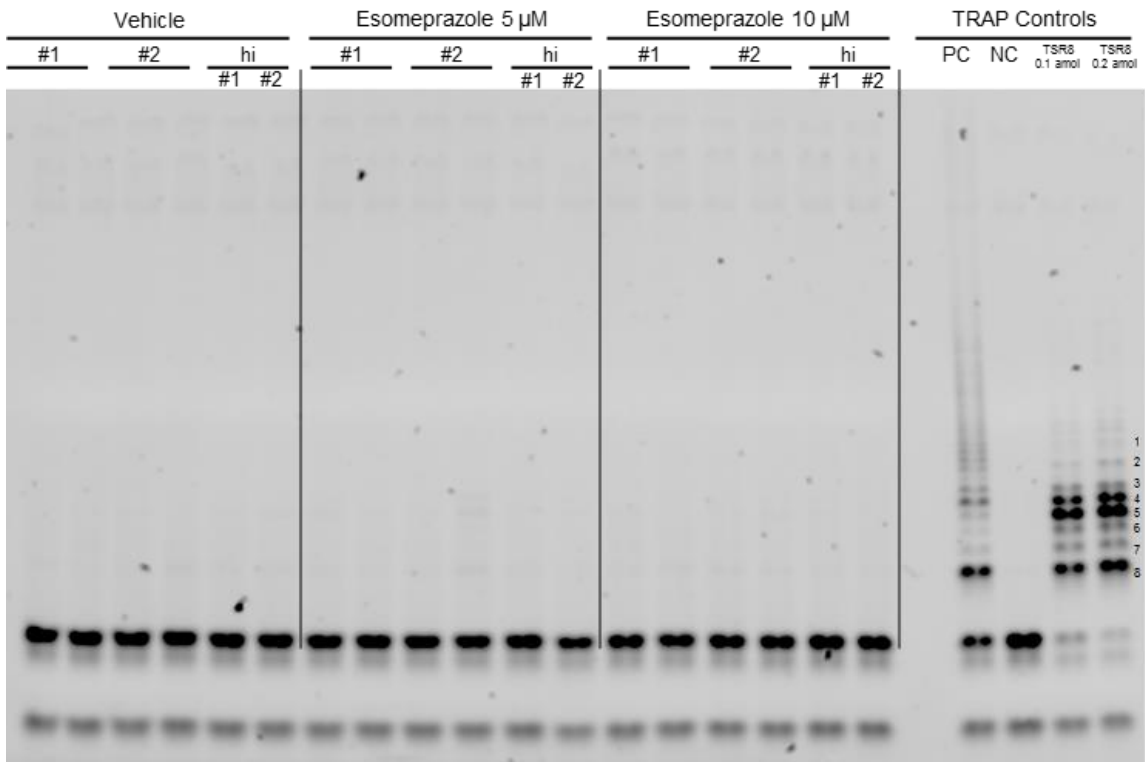
Online table I

gene symbol	gene name	function
AGTR1	angiotensin II receptor type 1	vasoconstriction
ALDH1A3	aldehyde dehydrogenase 1 family member A3	detoxification of aldehydes produced during lipid peroxidation and alcohol metabolism
ANGPT1	angiopoietin 1	secreted glycoprotein that inhibits endothelial permeability and contributes to blood vessel maturation and stability, and may be involved in early development of the heart
ANPEP	alanyl (membrane) aminopeptidase	plays a role in the final digestion of peptides generated from hydrolysis of proteins by gastric and pancreatic proteases
COL1A1	collagen, type I, alpha 1	a fibril-forming collagen found in most connective tissues and is abundant in bone, cornea, dermis and tendon
COL1A2	collagen type 1, alpha 2	fibril-forming collagen found in most connective tissues and is abundant in bone
COL3A1	collagen type 3, alpha 1	fibrillar collagen that is found in extensible connective tissues such as skin, lung, uterus, intestine and the vascular system, frequently in association with type I collagen
COL4A3	collagen, type IV, alpha 3 (Goodpasture	the major structural component of basement membranes
COL5A2	collagen type V alpha 2	regulate the assembly of heterotypic fibers composed of both type I and type V collagen
CXCL1	chemokine (C-X-C motif) ligand 1 (melanoma growth stimulating activity,	plays a role in inflammation and as a chemoattractant for neutrophils
CXCL10	chemokine (C-X-C motif) ligand 10	Binding to CXCR3 results in pleiotropic effects, including stimulation of monocytes, natural killer and T-cell migration, and modulation of adhesion molecule expression
CXCL8	chemokine (C-X-C motif) ligand 8	chemoattractant and a potent angiogenic factor
DCN	decorin	binds to type I collagen fibrils, and plays a role in matrix assembly
DLX2	distal-less homeobox 2	postulated to play a role in forebrain and craniofacial development
EDNRA	endothelin receptor type A	receptor for endothelin-1, a potent vasoconstrictor
EGF	epidermal growth factor	a potent mitogenic factor that plays an important role in the growth, proliferation and differentiation of numerous cell types
EGFR	epidermal growth factor receptor	cell proliferation and angiogenesis
ERBB3	erb-b2 receptor tyrosine kinase 3	cell to cell communication and cell proliferation or differentiation
F3	coagulation factor III (thromboplastin, tissue factor)	cell surface glycoprotein that enables cells to initiate the blood coagulation cascades (it functions as the high-affinity receptor for the coagulation factor VII)
FGF1	fibroblast growth factor 1	functions as a modifier of endothelial cell migration and proliferation, as well as an angiogenic factor
GNG11	guanine nucleotide binding protein (G protein), gamma 11	transmembrane signaling
ICAM1	intercellular adhesion molecule 1	cell surface glycoprotein
IFNA1	interferon, alpha 1	produced by macrophages and has antiviral activity
IGFBP3	insulin-like growth factor binding protein 3	it binds to IGFs in the plasma prolonging the half-life of IGFs and altering their interaction with cell surface receptors
IL11	interleukin 11	stimulate the T-cell-dependent development of immunoglobulin-producing B cells. It also support the proliferation of hematopoietic stem cells and megakaryocyte progenitor cells.
IL1B	interleukin 1, beta	pro-inflamatory cytokine
IL6	interleukin 6	pro-inflamatory cytokine
ILK	integrin linked kinase	plays a role in epithelial to mesenchymal transition and implicated in tumor growth and metastasis
KRT19	keratin 19, type I	responsible for structural integrity of epithelial cells
LECT1	leukocyte cell derived chemotaxin 1	inhibits angiogenesis and promotes chondrocyte growth
MMP1	matrix metallopeptidase 1 (interstitial	breakdown of extracellular matrix (collagens, types I, II, and III)
MMP9	matrix metalooprotase 3	involved in wound repair and progression of atherosclerosis
NOG	noggin	binds and inactivates members of TGF-beta superfamily signaling proteins, such as BMP4. It also appears to have a pleiotropic effect
NPPB	natriuretic peptide B	natriuresis, diuresis, vasorelaxation, inhibition of renin and aldosterone secretion, and a key role in cardiovascular homeostasis.

PDGFRA	platelet-derived growth factor receptor, alpha polypeptide	role in organ development, wound healing, and tumor progression
PLAU	plasminogen activator, urokinase	degradation of the extracellular matrix, possible tumor cell migration and associated with late-onset Alzheimer disease
PLEK2	pleckstrin 2	involved in cytoskeletal reorganization
SELE	selectin E	mediates rolling of endothelial cells
SERPINB2	serpin peptidase inhibitor, clade B (ovalbumin), member 2 or plasminogen activator inhibitor type 2	Also called placental PAI. Expressed in detectable range during pregnancy. Cause for fibrosis during pregnancy
SERPINE1	serpin peptidase inhibitor, clade E (nexin, plasminogen activator inhibitor type 1), member 1	inhibitor of tissue plasminogen activator (tPA) and urokinase (uPA), and hence is an inhibitor of fibrinolysis (high concentrations of the gene product are associated with thrombophilia)
SMAD3	SMAD family member 3	transcriptional modulator activated by TGF-beta
SOD2	superoxide dismutase 2, mitochondrial	Responsible to clear mitochondrial reactive oxygen species (ROS)
SPP1	secreted phosphoprotein 1	causes pro-inflammatory responses
TBX2	T-box 2	role in tumorigenesis as an immortalizing agent
TGFBI	Transforming growth factor, beta-induced	induced by TGF-beta and acts to inhibit cell adhesion
THBS2	thrombospondin 2	mediates cell-to-cell and cell-to-matrix interactions and is a potent inhibitor of tumor growth and angiogenesis
TNF	tumor necrosis factor	pro-inflamatory cytokine
TWIST1	Twist homolog 1	transcription factor involved in regulation of endothelial to mesenchymal transition
VCAN1	versican	important role in cell adhesion, proliferation, migration and angiogenesis
WNT5A	wingless-type MMTV integration site family, member 5A	regulate developmental pathway during embryogenesis
WNT5B	wingless-type MMTV integration site family, member 5A	regulate developmental pathway during embryogenesis
ZEB2	zinc finger E-box binding homeobox 2	transcriptional repressor that interacts with activated SMADs

Online table II

gene symbol	gene name	function
ACE	angiotensin I converting enzyme	conversion of angiotensin I into angiotensin II
ADGRB1	Adhesion G Protein-Coupled Receptor B1	inhibitor of angiogenesis and a growth suppressor of glioblastomas
AMH	anti-Mullerian hormone	causes the regression of Mullerian ducts which would otherwise differentiate into the uterus and fallopian tubes
ANG	angiogenin, ribonuclease, RNase A family, 5	potent mediator of new blood vessel formation
APOE	apolipoprotein E	a main apoprotein of the chylomicron, binds to a specific receptor on liver cells and peripheral cells facilitating chylomicron uptake
BMP2	bone morphogenetic protein 2	induces bone and cartilage formation
BMP4	bone morphogenetic protein 4	plays an important role in the onset of endochondral bone formation in humans
CDKN1B	cyclin-dependent kinase inhibitor 1B (p27, Kip1)	binds to and prevents the activation of cyclin E-CDK2 or cyclin D-CDK4 complexes, and thus controls the cell cycle progression at G1. The degradation of this protein is required for the cellular transition from quiescence to a proliferative state.
CDKN1C	cyclin-dependent kinase inhibitor 1C (p57, Kip2)	Cell proliferation inhibitor and important tumorigenic gene
CHRD	chordin	dorsalizes early vertebrate embryonic tissues by binding to ventralizing TGF-beta-like bone morphogenetic proteins and sequestering them in latent complexes
COL18A1	collagen, type XVIII, alpha 1	may play an important role in retinal structure and in neural tube closure
CX3CL1	chemokine (C-X3-C motif) ligand 1	promotes strong adhesion of leukocytes to activated endothelial cells
DSC2	desmocollin 2	constitute the adhesive proteins of the desmosome cell-cell junction and are required for cell adhesion and desmosome formation
DSP	desmoplakin	obligate component of functional desmosomes that anchors intermediate filaments to desmosomal plaques
EDN2	endothelin 2	secretory vasoconstrictive peptide
EFNA1	ephrin-A1	mediating developmental events, especially in the nervous system and in erythropoiesis
EFNB2	ephrin-B2	mediating developmental events, especially in the nervous system and in erythropoiesis
EGFR	epidermal growth factor receptor	associated with cell proliferation
F11R	F11 receptor	important regulator of tight junction assembly in epithelia
FGF2	fibroblast growth factor 2	limb and nervous system development, wound healing, and tumor growth (possess broad mitogenic and angiogenic activities)
FGFR3	fibroblast growth factor receptor 3	plays a role in bone development and maintenance
FIGF	C-Fos Induced Growth Factor (Vascular Endothelial Growth Factor D)	is active in angiogenesis, lymphangiogenesis, and endothelial cell growth
FN1	fibronectin 1	involved in cell adhesion and migration processes including embryogenesis, wound healing, blood coagulation, host defense, and metastasis
FST	follistatin	inhibits follicle-stimulating hormone release
GADD45B	growth arrest and DNA-damage-inducible, beta	binding and activating MTK1/MEKK4 kinase, which is an upstream activator of both p38 and JNK MAPKs
GDF3	growth differentiation factor 3	regulators of cell growth and differentiation in both embryonic and adult tissues
GDF7	growth differentiation factor 7	regulate diverse processes in growth, repair and embryonic development

ID1	inhibitor of DNA binding 1, dominant negative helix-loop-helix protein	has no DNA binding activity but can inhibit the DNA binding and transcriptional activation ability of basic helix-loop-helix proteins with which it interacts
ID2	inhibitor of DNA binding 2, dominant negative helix-loop-helix protein	inhibit the functions of basic helix-loop-helix transcription factors in a dominant-negative manner by suppressing their heterodimerization partners through the HLH domains
INHBB	inhibin, beta B	a pituitary FSH secretion inhibitor
KIT	v-kit Hardy-Zuckerman 4 feline sarcoma viral oncogene homolog	type 3 transmembrane receptor for MGF (mast cell growth factor, also known as stem cell factor)
MDK	midkine (neurite growth-promoting factor 2)	promotes cell growth, migration, and angiogenesis, in particular during tumorigenesis
MSN	moesin	signaling for cell-cell recognition and cell movement
NODAL	nodal growth differentiation factor	may be essential for mesoderm formation and subsequent organization of axial structures in early embryonic development
NOS3	nitric oxide synthase 3 (endothelial cell)	Nitric oxide synthesis in endothelial cells
NPR1	natriuretic peptide receptor 1	natriuresis, diuresis, vasorelaxation, inhibition of renin and aldosterone secretion, and a key role in cardiovascular homeostasis.
NUDT13	nudix (nucleoside diphosphate linked moiety X)-type motif 13	hydrolase activity, metal ion binding (is localized in the mitochondrion)
PDGFRB	platelet-derived growth factor receptor, beta polypeptide	receptor for platelet-derived growth factor, and this growth factor is a mitogen for cells of mesenchymal origin
STAT1	signal transducer and activator of transcription 1	a transcription activator promoting cell viability
TFPI	tissue factor pathway inhibitor (lipoprotein-associated coagulation inhibitor)	protease inhibitor that regulates the tissue factor (TF)-dependent pathway of blood coagulation.
TFPI2	tissue factor pathway inhibitor 2	inhibit a variety of serine proteases including factor VIIa/tissue factor, factor Xa, plasmin, trypsin, chymotrypsin and plasma kallikrein. It is also identified as a tumor suppressor gene
TGFA	transforming growth factor, alpha	activates a signaling pathway for cell proliferation, differentiation and development
TGFB2	transforming growth factor, beta 2	regulate proliferation, differentiation, adhesion and migration
TIE1	tyrosine kinase with immunoglobulin-like and EGF-like domains 1	inhibiting angiopoietin 1 signaling through the endothelial receptor tyrosine kinase Tie2
TIMP3	TIMP metallopeptidase inhibitor 3	inhibitor of the matrix metalloproteinases
TMEM132A	transmembrane protein 132A	may play a role in embryonic and postnatal development of the brain. Increased resistance to cell death induced by serum starvation in cultured cells
TNFSF10	tumor necrosis factor (ligand) superfamily, member 10	pro-inflamatory cytokine
VCAM1	vascular cell adhesion molecule 1	mediates leukocyte-endothelial cell adhesion and signal transduction
VWF	von Willebrand factor	antihemophilic factor carrier and a platelet-vessel wall mediator in the blood coagulation system